

Mechanistic Studies on 14-Electron Ruthenacyclobutanes: Degenerate Exchange with Free Ethylene

Patricio E. Romero and Warren E. Piers*

Contribution from the University of Calgary, 2500 University Drive N.W.,
Calgary, Alberta, Canada T2N 1N4

Received October 20, 2006; E-mail: wpiers@ucalgary.ca

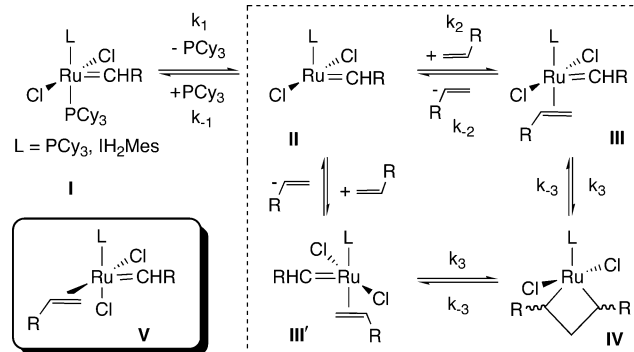
Abstract: The phosphonium alkylidene $[(\text{NHC})\text{Cl}_2\text{Ru}=\text{CH}(\text{PCy}_3)]^+[\text{B}(\text{C}_6\text{F}_5)_4]^-$, **1**, (NHC = *N*-heterocyclic carbene, Cy = cyclohexyl, C_6H_{11}) reacts with 2.2 equiv of ethylene at -50°C to form the 14-electron ruthenacyclobutane $(\text{NHC})\text{Cl}_2\text{Ru}(\text{CH}_2\text{CH}_2\text{CH}_2)$, **2**. NMR spectroscopic data indicates that **2** has a C_{2v} symmetric structure with a flat, kite shaped ruthenacyclobutane ring with significant C_α - C_β agostic interactions with the Ru center. Intramolecular exchange of C_α and C_β is fast ($14(2)\text{ s}^{-1}$ at 223 K) as measured by EXSY spectroscopy. Intermolecular exchange of C_α and C_β with the methylene groups of free ethylene is much slower and first order in both $[\text{Ru}]$ and $[\text{H}_2\text{C}=\text{CH}_2]$ ($4.8(3) \times 10^{-4}\text{ M}^{-1}\text{ s}^{-1}$). Activation parameters for this process are $\Delta H^\ddagger = 13.2(5)\text{ kcal mol}^{-1}$ and $\Delta S^\ddagger = -15(2)\text{ cal mol}^{-1}\text{ K}^{-1}$, also consistent with a rate limiting associative substitution as the key step in this exchange process. On the basis of this observation, mechanisms for the intermolecular exchange process are proposed and the implications for the mechanism of the propagation steps in catalytic olefin metathesis as mediated by Grubbs catalysts are discussed.

Introduction

Olefin metathesis is a powerful method for the equilibration of carbon-carbon double bonds that has been applied to a wide range of synthetic problems.¹ The high barrier to this process requires the use of a catalyst, and the evolution of today's state-of-the-art catalyst systems represent a pinnacle of achievement in catalyst development and optimization.² In particular, the ruthenium-based alkylidenes collectively known as the Grubbs type catalysts,^{3,4} **I**, are an amazingly versatile group of olefin metathesis mediators whose functional group tolerance and ease of handling has led to their widespread use in both academia and industry, in organic, polymer, and materials synthesis.¹

Since their initial discovery, extensive mechanistic studies have delivered a detailed understanding of their mode of

Scheme 1



operation (Scheme 1).⁵ In brief, the initiation step involves the loss of the dative phosphine ligand PCy₃ trans to L to yield a 14-electron alkylidene intermediate **II**. This highly reactive species either recoordinates PCy₃ to reform **I**, or picks up a substrate olefin, forming an olefin-alkylidene **III** that rapidly forms a formally Ru(IV) ruthenacyclobutane, **IV**. The relative rates of reaction of the active alkylidene with PR₃ versus olefin is strongly influenced by the nature of the remaining ligand L.^{5b} Collapse of the ruthenacyclobutane intermediate in the opposite sense of its formation gives **III'** (this has the same structure as **III** in a degenerate metathesis as shown, but is different in productive metathesis reactions) consummating the metathesis double bond rearrangement and regenerating **II** upon loss of product olefin.

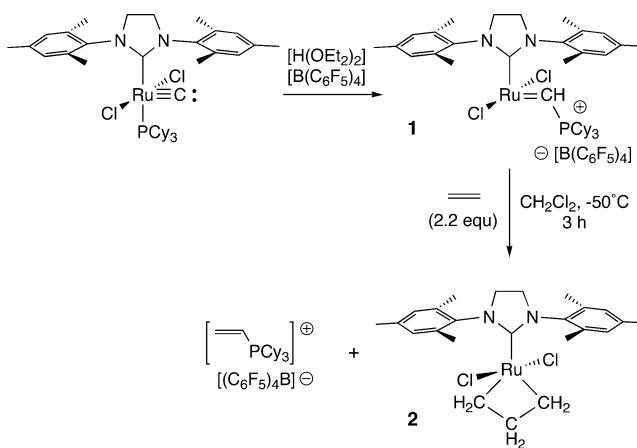
- (1) (a) Grubbs, R. H., Ed. *Handbook of Metathesis*; Wiley-VCH: Weinheim, Germany, 2003. (b) Conrad, J. C.; Fogg, D. E. *Curr. Org. Chem.* **2006**, *10*, 185.
- (2) (a) Schrock, R. R.; Hoveyda, A. H. *Angew. Chem., Int. Ed.* **2003**, *42*, 4592. (b) Trnka, T. M.; Grubbs, R. H. *Acc. Chem. Res.* **2001**, *34*, 18. (c) Schrock, R. R. *Angew. Chem., Int. Ed.* **2006**, *45*, 3748. (d) Grubbs, R. H. *Angew. Chem., Int. Ed.* **2006**, *45*, 3760.
- (3) (a) Schwab, P.; Grubbs, R. H.; Ziller, J. W. *J. Am. Chem. Soc.* **1996**, *118*, 100. (b) Schwab, P.; France, M. B.; Ziller, J. W.; Grubbs, R. H. *Angew. Chem., Int. Ed. Engl.* **1995**, *34*, 2039. (c) Schöll, M.; Trnka, T. M.; Morgan, J. P.; Grubbs, R. H. *Tetrahedron Lett.* **1999**, *40*, 2247. (d) Kingsbury, J. S.; Harrity, J. P. A.; Bonitatebus, P. J., Jr.; Hoveyda, A. H. *J. Am. Chem. Soc.* **1999**, *121*, 791. (e) Weskamp, T.; Schattenmann, W. C.; Spiegler, M.; Herrmann, W. A. *Angew. Chem., Int. Ed.* **1998**, *37*, 2490. (f) Herrmann, W. A. *Angew. Chem., Int. Ed.* **1999**, *38*, 262. (g) Huang, J.; Stevens, E. D.; Nolan, S. P.; Peterson, J. L. *J. Am. Chem. Soc.* **1999**, *121*, 2674.
- (4) Successful modifications of the Grubbs framework: (a) Wakamatsu, H.; Blechert, S. *Angew. Chem., Int. Ed.* **2002**, *41*, 794. (b) Grela, K.; Harutyunyan, S.; Michrowska, A. *Angew. Chem., Int. Ed.* **2002**, *41*, 4038. (c) Krause, J. O.; Nuyken, O.; Wurst, K.; Buchmeiser, M. R. *Chem.-Eur. J.* **2004**, *10*, 777. (d) Conrad, J. C.; Parnas, H. H.; Snelgrove, J. L.; Fogg, D. E. *J. Am. Chem. Soc.* **2005**, *127*, 11882. (e) Bieniek, M.; Bujok, R.; Cabaj, M.; Lukan, N.; Lavigne, G.; Arlt, D.; Grela, K. *J. Am. Chem. Soc.* **2006**, *128*, 13652.

- (5) (a) Dias, E. L.; Nguyen, S. T.; Grubbs, R. H. *J. Am. Chem. Soc.* **1997**, *119*, 3887. (b) Sanford, M. S.; Love, J. A.; Grubbs, R. H. *J. Am. Chem. Soc.* **2001**, *123*, 6543.

While the gross features of the mechanism are well established, the precise structures of the proposed intermediates, and the intimate details concerning the mechanisms of the interconversions “inside the box” remain largely obscure. The bulk of the catalyst in these systems exists in the 16-electron PCy₃ coordinated form **I**, such that the active 14- and 16-electron intermediates are invisible to most spectroscopic techniques. Mass spectrometry has provided evidence for their existence⁶ but sheds little light on their structures. Computational studies have contributed the most significantly to our understanding of the intermediate structures,⁷ but experimental evidence in support of these proposals has been, until recently, difficult to come by. That which has been uncovered is in some cases contradictory; for example model compounds for the olefin-alkylidene adduct in some instances indicate bottom face coordination as depicted inside the box,⁸ and in others a side-on pathway, **V** (inset, Scheme 1),⁹ in which the chloride ligands assume a cis geometry, has been observed. These observations indicate that the energy surface connecting these species is quite shallow and sensitive to even slight modifications in ligand environment and reaction medium.^{7e} It is clear that a more detailed understanding of the structures associated with these intermediates and the intimate mechanisms of their interconversion is critical for the design of more active, longer-lived, and selective catalysts.

Recent discoveries in our laboratories have provided access to 14-electron phosphonium alkylidenes¹⁰ and ruthenacyclobutanes¹¹ of direct relevance to olefin metathetical processes catalyzed by Grubbs type catalysts. Specifically, and surprisingly, we found that protonation of the ruthenium carbides first reported by Heppert¹² resulted in a migration of a phosphine ligand (trans to L) from ruthenium to the newly formed methylidyne carbon (Scheme 2). The mechanism of this migration and the reasons why protonation of the carbide triggers this transformation are unclear, but the product, **1**, is a 14-electron phosphonium alkylidene that models the presumed active species formed upon phosphine dissociation in the Grubbs catalyst precursor. These compounds are air and moisture stable, retaining many of the convenient features of the parent Grubbs systems, and feature a significantly lower barrier entry into the 14-electron alkylidenes responsible for the bulk of metathesis

Scheme 2



activity. As such, they are among the fastest initiating Grubbs-type catalysts known.¹³

In addition to fast initiation, catalyst **1** is ideal for the direct study of the ruthenacyclobutanes formed during metathesis via stoichiometric reactions with simple olefins such as ethylene¹¹ and propylene.¹⁴ Experimentally accessed details concerning the structure, dynamic behavior and reactivity of these crucial intermediates are now emerging. The clean generation of the parent ruthenacyclobutane **2** has allowed us to begin to study its chemistry, specifically chemistry relevant to the propagating step in olefin metathesis. Herein, we report kinetic studies on the exchange of free ethylene with the metallacyclobutane methylene units, which provide evidence for an associative exchange mechanism in this parent system.

Results and Discussion

Synthesis and Structure of Ruthenacyclobutane 2. Reaction of **1** (the counteranion = [B(C₆F₅)₄]⁻ in all of these studies) with a small excess of ethylene at -50 °C results in expulsion of the vinyl phosphonium salt [(CH₂=CH)PCy₃]⁺[B(C₆F₅)₄]⁻ and clean formation of the parent, unsubstituted ruthenacyclobutane **2** (Scheme 2).¹¹ The ¹H and ¹³C NMR data for **2**, and that of a related compound incorporating an unsymmetrically N-arylated N-heterocyclic carbene (NHC) ligand,¹⁴ strongly implicate the TBP geometry shown. The chlorides occupy the axial positions of the trigonal bipyramid, while the ruthenacyclobutane lies underneath the NHC ligand such that the plane of the RuC₃ ring is co-incident with that of the C₃N₂ wingspan of the NHC ligand.

When contrasted with known ruthenacyclobutanes in particular,¹⁵ and with typical platinum group metallacyclobutanes in general,¹⁶ the chemical shifts for the proton and carbon nuclei of **2** are highly unusual. For example, H_α (δ 6.62 ppm) appears downfield of H_β (δ -2.65 ppm) corresponding to Δδ(H_{α-β}) = 9.27 ppm, while an analogous but more marked trend is observed in the ¹³C NMR with C_α (δ 94.0 ppm) and C_β (δ 2.30

- (6) (a) Hinderling, C.; Adlhart, C.; Chen, P. *Angew. Chem., Int. Ed.* **1998**, *37*, 2685. (b) Adlhart, C.; Hinderling, C.; Baumann, H.; Chen, P. *J. Am. Chem. Soc.* **2000**, *122*, 8204. (c) Adlhart, C.; Volland, M. A. O.; Hofmann, P.; Chen, P. *Helv. Chim. Acta* **2000**, *83*, 3306. (d) Adlhart, C.; Chen, P. *Helv. Chim. Acta* **2000**, *83*, 2192.
- (7) (a) Adlhart, C.; Chen, P. *J. Am. Chem. Soc.* **2004**, *126*, 3496. (b) Cavallo, L. *J. Am. Chem. Soc.* **2002**, *124*, 8965. (c) Correa, A.; Cavallo, L. *J. Am. Chem. Soc.* **2006**, *128*, 13352. (d) Aagaard, O. M.; Meier, R. J.; Buda, F. *J. Am. Chem. Soc.* **1998**, *120*, 7174. (e) Benitez, D.; Goddard, W. A., III. *J. Am. Chem. Soc.* **2005**, *127*, 12218. (f) Straub, B. F. *Angew. Chem., Int. Ed.* **2005**, *44*, 5974. (g) Suresh, C. H.; Baik, M.-H. *J. Chem. Soc., Dalton Trans.* **2005**, 2982. (h) Suresh, C. H.; Koga, N. *Organometallics* **2004**, *23*, 76. (i) Fomine, S.; Vargas, S. M.; Tlenkopatchev, M. A. *Organometallics* **2003**, *22*, 93. (j) Vyboishchikov, S. F.; Buhl, M.; Thiel, W. *Chem.—Eur. J.* **2002**, *8*, 3962.
- (8) Tallarico, J. A.; Bonitatebus, P. J., Jr.; Snapper, M. L. *J. Am. Chem. Soc.* **1997**, *119*, 7157.
- (9) (a) Ung, T.; Hejl, A.; Grubbs, R. H.; Schrodi, Y. *Organometallics* **2004**, *23*, 5399. (b) Anderson, D. R.; Hickstein, D. D.; O’Leary, D. J.; Grubbs, R. H. *J. Am. Chem. Soc.* **2006**, *128*, 8386.
- (10) (a) Romero, P. E.; Piers, W. E.; McDonald, R. *Angew. Chem., Int. Ed.* **2004**, *43*, 6161. (b) Dubberley, S. R.; Romero, P. E.; Piers, W. E.; McDonald, R.; Parvez, M. *Inorg. Chim. Acta* **2006**, *359*, 2658.
- (11) Romero, P. E.; Piers, W. E. *J. Am. Chem. Soc.* **2005**, *127*, 5032.
- (12) (a) Carlson, R. G.; Gile, M. A.; Heppert, J. A.; Mason, M. H.; Powell, D. R.; Vander Velde, D.; Vilain, J. M. *J. Am. Chem. Soc.* **2002**, *124*, 1580. See also: (b) Caskey, S. R.; Stewart, M. H.; Kivela, J. E.; Sootsman, J. R.; Johnson, M. J. A.; Kampf, J. W. *J. Am. Chem. Soc.* **2005**, *127*, 16750.

- (13) (a) Wakamatsu, H.; Blechert, S. *Angew. Chem., Int. Ed.* **2002**, *41*, 2403. (b) Love, J. A.; Morgan, J. P.; Trnka, T. M.; Grubbs, R. H. *Angew. Chem., Int. Ed.* **2002**, *41*, 4035.
- (14) Wenzel, A. G.; Grubbs, R. H. *J. Am. Chem. Soc.* **2006**, *128*, 16048.
- (15) (a) Andersen, R. A.; Jones, R. A.; Wilkinson, G. *J. Chem. Soc., Dalton Trans.* **1978**, 446. (b) Statler, J. S.; Wilkinson, G.; Thornton-Pett, M.; Hursthouse, M. B. *J. Chem. Soc., Dalton Trans.* **1984**, 1731. (c) Diversi, P.; Ingrosso, G.; Lucherini, A.; Marchetti, F.; Adovasio, V.; Nardelli, M. *J. Chem. Soc., Dalton Trans.* **1991**, 203. (d) McNeill, K.; Andersen, R. A.; Bergman, R. G. *J. Am. Chem. Soc.* **1997**, *119*, 11244.
- (16) Jennings, P. W.; Johnson, L. L. *Chem. Rev.* **1994**, *94*, 2241.

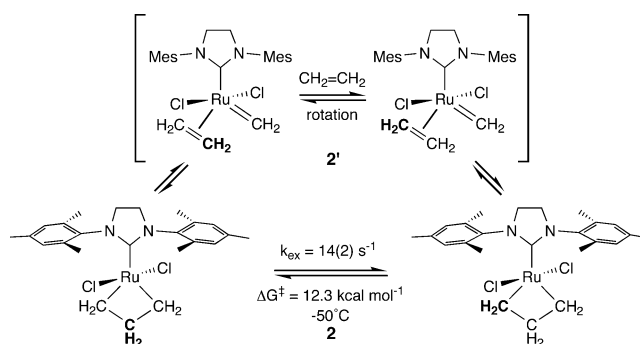
ppm), with a $\Delta\delta(C_{\alpha-\beta}) = 91.7$ ppm. Comparative data for other related metallacyclobutanes are collected in Table S1 in the Supporting Information, and show that in most cases the H_{α} and C_{α} resonances appear substantially *upfield* of those for H_{β} and C_{β} , the opposite to what is observed for **2**. Furthermore, the differences in the chemical shifts are far less pronounced. Notably, however, the late metal metallacyclobutanes presented for comparison are all either 18- or 16-electron species and do not provide entry into olefin metathesis catalytic cycles. In contrast, the trends and positions for the $^1H/^{13}C$ NMR resonances in **2** are reproduced in several more electron deficient early metal (and metathesis active) titana- and tungstenacyclobutanes (see data in Table S2). For these metallacyclobutanes, 1H NMR spectroscopy data show that in general, the H_{β} resonance appears at ~ 0 ppm, well separated and upfield from H_{α} which is found at $\sim 4 \pm 1$ ppm. ^{13}C NMR spectroscopy reveals a similar but even more manifest trend: the C_{β} resonance is found ~ 100 ppm upfield of the C_{α} resonance. The trend $C_{\alpha} > C_{\beta}$ and $H_{\alpha} > H_{\beta}$ is followed by every single example in Table S2, regardless of metal, substitution at the ring, and oxidation state, although the tantalum and tungsten complexes bearing unsubstituted metallarings (entries 6 and 7) show closer resemblance to the values obtained for **2**. Schrock and co-workers have observed that for group 6 metallacyclobutanes (entries 7–9) the unusual chemical shifts are associated with trigonal bipyramidal (TBP) structures featuring short $M \cdots C_{\beta}$ interactions, both in solution and in the solid state.¹⁷

Although we do not have specific structural data for **2** (i.e., the $M \cdots C_{\beta}$ distance), the similarity in NMR data to the data of those metallacyclobutanes that do feature this interaction suggests that the ruthenacyclobutane ring in **2** features a relatively flat, kite-shaped geometry in which $C_{\alpha}-C_{\beta}$ agostic interactions stabilize the compound, drawing C_{β} closer to the metal. Computed structures of **2** and related species support this notion, with distances of 2.266 Å reported in recent studies.^{7g,h} Furthermore, the observed CH and CC coupling constants within the ruthenacyclobutane moiety in **2** are fully consistent with this bonding picture. In a recent detailed spectroscopic and structural study by Ernst and co-workers, the issue of $(C-C) \cdots M$ agostic interactions in electron deficient systems was addressed and $^1J(^{13}C-^{13}C)$ values were invoked as a primary metric of their presence.¹⁸ Many of the systems evaluated were titanacyclobutanes derived from Tebbe's reagent, for which $^1J(^{13}C-^{13}C)$ values of 21–24 Hz were extracted. $^1J(^{13}C-^{13}C)$ coupling constants of 30–39 Hz are normal for C–C single bonds, while values of ~ 29 Hz are typically observed for cyclobutanes. Ernst and co-workers also found that $(C-C) \cdots M$ agostic interactions not only are expressed in terms of low $^1J(^{13}C-^{13}C)$ but also in unusually high accompanying $^1J_{C-H}$ for the bond in question (149–167 Hz). Spectroscopic analysis of the isotopically enriched **2**- $^{13}C_3$ showed values of $^1J(^{13}C-^{13}C) = 15.0$ Hz and $^1J_{C-H} = 165.4$ (H_{α}), 154.8 (H_{β}) Hz, lending strong support for the presence of C–C agostic interactions in **2**, stabilizing the electron deficient 14-electron Ru center. Indeed, the observed $^1J(^{13}C-^{13}C)$ for **2** is among the lowest values observed to date, suggesting this interaction is significant in **2**. This presents another example of a significant role for agostic interactions in stabilizing highly reactive organometallic intermediates in

(17) Feldman, J.; Schrock, R. R. *Prog. Inorg. Chem.* **1991**, *39*, 1.

(18) Harvey, B. G.; Mayne, C. L.; Arif, A. M.; Ernst, R. D. *J. Am. Chem. Soc.* **2005**, *127*, 16426.

Scheme 3



important catalytic cycles.¹⁹ In the case of **2**, and perhaps other metathesis active metallacycles, these interactions serve to not only to stabilize the metallacycles, but also to bias it toward the C–C activation chemistry that is a necessary step in olefin metathesis. What remains to be seen is how important these interactions are in other, substituted ruthenacyclobutanes more relevant to productive olefin metathesis. Early indications are that, for the Grubbs type catalysts, C_{2v} -like structures akin to that observed for the parent **2** are also present in such intermediates;¹⁴ further studies are currently in progress to probe the generality of these structural phenomena.

Ethylene Exchange Studies. Clean samples of compound **2** can be generated conveniently at temperatures at or below -50 °C from pure **1** and stoichiometric ethylene (2.2 equiv); these samples retain their spectral integrity in the presence or absence of excess ethylene up to temperatures of -25 °C. Warming above this temperature results in decomposition via an unknown mechanism,²⁰ where propene is the primary product arising from the three carbons of the ruthenacyclobutane fragment (as determined by ^{13}C NMR spectroscopy from the decomposition of **2**- $^{13}C_3$). Although the ground state structure of **2** is clearly a ruthenacyclobutane, dynamic NMR studies performed independently by Wenzel and Grubbs¹⁴ and us indicate that exchange of the α -methylenes and the β - CH_2 group is rapid on the NMR time scale. Using EXSY experiments,^{21,22} we find that the rate of exchange between H_{α} and H_{β} at 223 K is $14(2) s^{-1}$; this compares well to a value of $26(2) s^{-1}$ at 230 K reported by Wenzel and Grubbs using the same methodology. Presumably, this exchange process reflects a rapid equilibrium between **2** and a higher energy olefin–methylidene intermediate (**2'**) that we do not observe spectroscopically (Scheme 3). This is in line with computational studies that indicate the barrier to interconversion of these two species is small, but that for the NHC ligated system, the ruthenacyclobutane isomer is favored thermodynamically.⁷

We have also observed a slower process involving exchange of the C_{α} and C_{β} methylene units of **2** with those of free ethylene, when present in excess. Although this process is slow on the NMR time scale, it becomes chemically apparent when **2**- $^{13}C_3$ is treated with an excess of unlabeled ethylene and the

(19) (a) Piers, W. E.; Bercaw, J. E. *J. Am. Chem. Soc.* **1990**, *112*, 9406. (b) Grubbs, R. H.; Coates, G. W. *Acc. Chem. Res.* **1996**, *29*, 85.

(20) van Rensburg, W. J.; Steynberg, P. J.; Meyer, J. H.; Kirk, M. M.; Forman, G. S. *J. Am. Chem. Soc.* **2004**, *126*, 14332.

(21) (a) Perrin, C. L.; Dwyer, T. J. *Chem. Rev.* **1990**, *90*, 935. (b) Ramachandran, R.; Knight, C. T. G.; Kirkpatrick, R. J.; Oldfield, E. *J. Magn. Reson.* **1985**, *65*, 136.

(22) This methodology has been used effectively to measure exchange rates in titanaazacyclobutanes: Polse, J. L.; Andersen, R. A.; Bergman, R. G. *J. Am. Chem. Soc.* **1998**, *120*, 13405.

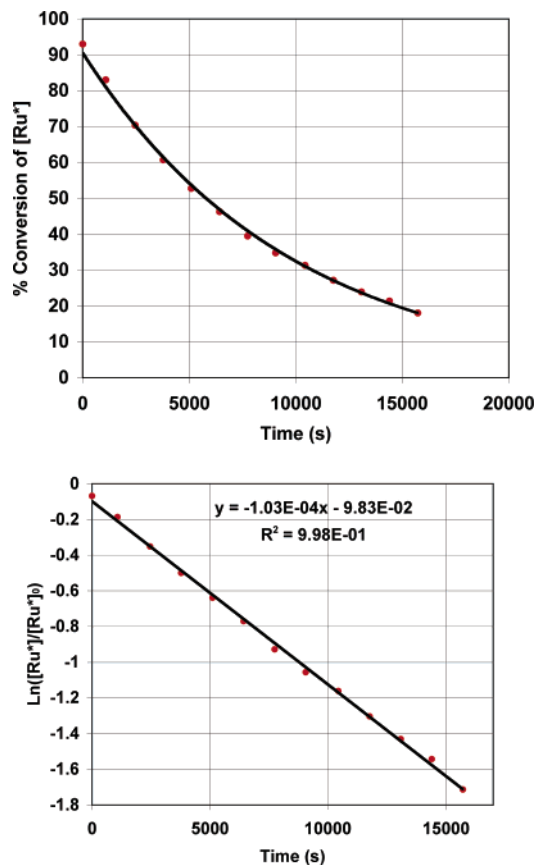


Figure 1. Representative speciation (top) and first order (bottom) plots for the decay of $2\text{-}^{13}\text{C}_3$ into **2** ($-40\text{ }^\circ\text{C}$, 30 equiv of $\text{CH}_2=\text{CH}_2$).

^{13}C label washes out of compound **2** over the course of 3–4 h. The mechanism of this process is directly relevant to the essential propagating steps in olefin metathesis as mediated by Grubbs catalysts, but until now has been kinetically invisible because of the rate determining initiation step involving phosphine dissociation in the commercially available catalysts. We therefore have performed a kinetic study on the degenerate exchange of ethylene into **2** in an effort to probe the mechanism in more detail.²³

Experiments were performed by generating a known amount of $2\text{-}^{13}\text{C}_3$ in a J-Young NMR tube at $-50\text{ }^\circ\text{C}$ via treatment of **1** with 2.2 equiv of $^{13}\text{CH}_2=^{13}\text{CH}_2$ for 2–3 h. Upon full conversion to $2\text{-}^{13}\text{C}_3$, a known excess of unlabeled ethylene (15–35 equiv) was admitted into the tube and the loss of label monitored over time. Speciation plots indicated clean exponential pseudo-first-order decay in labeled **2** (Figure 1) over at least three half-lives, indicating the reaction is first order in ruthenacyclobutane. The order in olefin concentration was determined from a plot of k_{obs} versus $[\text{CH}_2=\text{CH}_2]$ over a range of 0.24–0.46 M at $-50\text{ }^\circ\text{C}$ (Figure 2). Although the concentration range is relatively narrow,²⁴ an excellent linear correlation between k_{obs} and $[\text{CH}_2=\text{CH}_2]$ was obtained, indicating that the reaction is also first order in ethylene over this concentration range. A rate constant for the ethylene exchange $k_{\text{inter}} = 4.8(3) \times 10^{-4}\text{ M}^{-1}\text{ s}^{-1}$ was obtained from the slope of the plot, confirming that this intermolecular exchange process is substantially slower (4 orders of magnitude) than the intramolecular exchange of C_α and C_β as discussed above.

The nonzero intercept of the plot in Figure 2 deserves some comment. The line cuts the x -axis of the plot at $[\text{CH}_2=\text{CH}_2] \approx$

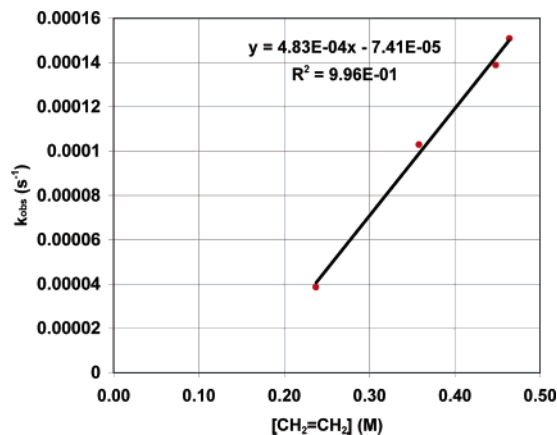


Figure 2. Plot of k_{obs} versus $[\text{CH}_2=\text{CH}_2]$ for the decay of $2\text{-}^{13}\text{C}_3$ into **2** at $-40\text{ }^\circ\text{C}$.

0.15 M, corresponding to roughly 10 equiv of ethylene. In fact, when less than 15 equiv of ethylene are employed in these experiments, the speciation diagrams analogous to that shown in Figure 1 (top) cannot be fit with a first-order decay treatment (see Figure S1 for an example). Under these conditions, the scrambling of label back in to **2** becomes competitive with the forward loss of label; in other words, true pseudo-first-order conditions do not apply. This is not uncommon in degenerate exchanging systems that are probed by isotopic labeling and is usually treated using the McKay equation²⁵ for approach to equilibrium kinetics to extract k_{obs} values. However, the system involving $2\text{-}^{13}\text{C}_3$ and $\text{CH}_2=\text{CH}_2$ described here is complicated by the involvement of additional species such as $^{13}\text{CH}_2=\text{CH}_2$ and $2\text{-}^{13}\text{C}_1$, for example, making the McKay equation inadequate for our purposes; we could not extract meaningful k_{obs} values using this treatment. Increasing the excess of unlabeled ethylene allowed access to a regime in which these complications became negligible, and while the x -intercept in Figure 2 has no clear kinetic meaning, it represents the ethylene concentration at the border between the “equilibrium zone” and the “pseudo-first-order zone” of the reaction where different kinetic regimes are operative.

What is clear from Figure 2, however, is that, at high enough concentrations of ethylene, the rate of exchange is dependent on $[\text{CH}_2=\text{CH}_2]$, indicating that the rate-limiting step in the process is *associative* in nature. This is corroborated by an Eyring treatment of rate data obtained at various temperatures using an ethylene concentration of 0.37 M (≈ 20 equiv). This was the optimal amount of ethylene to ensure that the same excess was present at all temperatures measured in the range -50 to $-20\text{ }^\circ\text{C}$, based on measured solubilities of ethylene in CD_2Cl_2 . Although the temperature range technically accessible in these experiments was quite narrow, a reasonable Eyring plot (Figure 3) was obtained, yielding the activation parameters $\Delta H^\ddagger = 13.2(5)\text{ kcal mol}^{-1}$ and $\Delta S^\ddagger = -15(2)\text{ cal mol}^{-1}\text{ K}^{-1}$. The negative sign of the activation entropy is consistent with an exchange mechanism that is associative in character.

(23) Experiments probing the reactivity of **2** with other olefins indicate that the parent ruthenacyclobutane is thermodynamically favored over substituted derivatives, even in the presence of excess olefin. Therefore, studying the kinetics of a nondegenerate exchange of olefin into **2**, although desirable, was not possible using this strategy.

(24) The solution was essentially saturated with ethylene at 0.46 M.

(25) Katakis, D.; Gordon, G. *Mechanisms of Inorganic Reactions*, 1st ed.; John Wiley & Sons: New York, 1987.

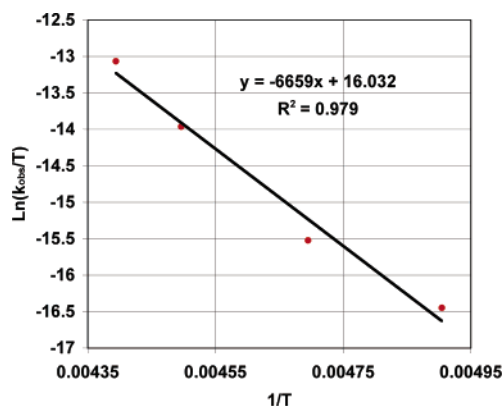
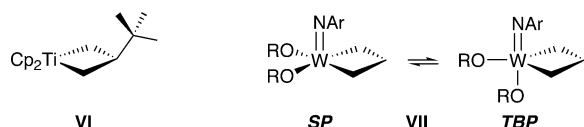


Figure 3. Eyring plot for the degenerate ethylene exchange of $2\text{-}^{13}\text{C}_3$ into 2 over the temperature range 204–228 K.

The observation of a clear [olefin] dependence on the rate of exchange of olefin into a metathesis active metallacyclobutane structure here contrasts with previous observations. For example, in a series of papers on such exchange processes in titanacyclobutanes, **VI**, Grubbs and co-workers report high enthalpic barriers on the order of 30 kcal mol^{-1} and positive entropies of activation around $9 \text{ cal mol}^{-1} \text{ K}^{-1}$,²⁶ while in Schrock type systems, exchanges of ethylene into tungstenacyclobutanes of general formula $(\text{RO})_2(\text{ArN})\text{W}(\text{CH}_2\text{CHRCH}_2)$, **VII**, are first order in metallacyclobutane and zero order in ethylene.²⁷ In the latter systems, activation enthalpies are $\approx 20 \text{ kcal mol}^{-1}$ for square pyramidal tungstenacyclobutanes and $25\text{--}30 \text{ kcal mol}^{-1}$ for trigonal bipyramidal geometries, whereas ΔS^\ddagger values are small and negative for the SP example and $11\text{--}23 \text{ cal mol}^{-1} \text{ K}^{-1}$ for the TBP systems.



In the olefin exchange process involving both of these families of catalysts, opening of the metallacyclobutane is rate determining, while substitutional exchange of ethylene for olefin in the resulting olefin–alkylidene complex is fast; the lack of dependence on [olefin] therefore sheds no light on the character of this step in the metathesis process. Intuitively, it seems likely that in these formally d^0 systems, dissociative processes would be operative, although in the more complex tungsten systems, the barrier between isomeration from TBP to SP geometries may be playing a significant role in the overall exchange process.

A comparison of the rates of intramolecular C_α and C_β exchange in 2 and intermolecular exchange of these carbons with those of free ethylene indicates that for this ruthenacyclobutane, opening of the ruthenacyclobutane to an ethylene–methylidene isomer ($2'$) is *not* the rate-limiting step in the reaction. This is consistent with the postulate that the ruthenacyclobutane ring in 2 features a short $\text{Ru}\cdots\text{C}_\beta$ interaction and strong $C_\alpha\text{--}C_\beta$ to metal agostic interactions, which should facilitate opening of the ring. The fact that these are, formally,

d^4 or d^6 systems means that the species $2'$ is more energetically favorable (and more likely a true intermediate) than its d^0 counterparts. Since the intermolecular ethylene exchange is now rate limiting, the dependence on [olefin] is revealed as first order, an associative exchange. At first glance, this may appear surprising, given that the initiation step in Grubbs catalysts, that is, intermolecular substitution of a PR_3 ligand by an olefin substrate, has been shown conclusively to be dissociative in nature.⁵ However, that study also points to the high affinity of the $(\text{NHC})\text{Cl}_2\text{Ru}=\text{CHR}$ fragment for olefin in comparison to the phosphine ligand; since our study pertains specifically to the highly “olefinophilic” generation 2 Grubbs framework, it stands to reason that the substitution mechanism may plausibly switch from dissociative to associative when $L = \text{olefin}$ versus PR_3 and not involve the high-energy 14-electron methylidene intermediate $(\text{NHC})\text{Cl}_2\text{Ru}=\text{CH}_2$.

While establishment of the associative character of this exchange allows for the elimination of ethylene dissociation from $2'$ as a mechanism, the precise nature of the exchange mechanism in terms of the structures of intermediates remains somewhat speculative. Two possibilities are presented in Schemes 4 and 5 that incorporate what is known from computational studies⁷ and previous experimental observations,^{6,8,9} while maintaining adherence to the principle of microscopic reversibility.²⁸ As a general comment, the processes depicted in the schemes assume that exchange proceeds from the ethylene–methylidene derivative $2'$. Mechanisms that are similar in character to those proposed but that stem directly from ruthenacyclobutane 2 are also possible, but keeping in mind that the two isomeric forms are in exchange at a much faster rate relative to that of intermolecular ethylene exchange, it is likely that ring-opened and -closed forms of the intermediates proposed are also rapidly interconverting. The higher energy $2'$ is likely more reactive than 2 and so the schemes depict exchange processes emanating from this structure.

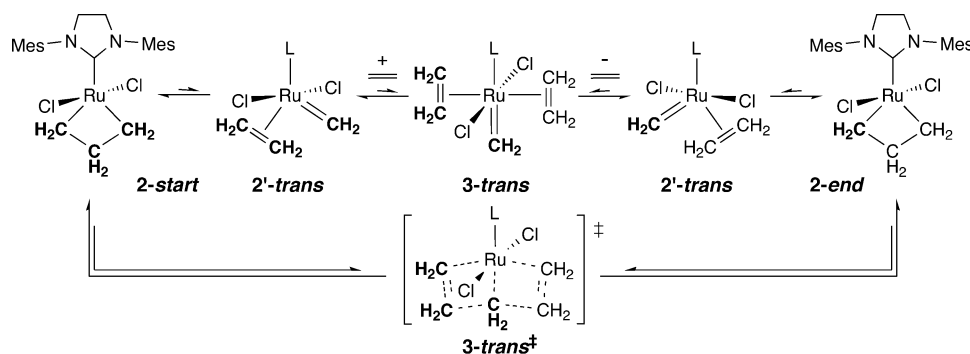
The two mechanisms are delineated by the geometry of the chloride ligands with respect to each other: trans disposed (Scheme 4) and cis arranged (Scheme 5). The bold CH_2 groups in these schemes represent ^{13}C labeled carbons. In Scheme 4, 2 opens to form $2'\text{-trans}$, which reacts associatively with ethylene to give the formally 18-electron species 3-trans , which may be an intermediate, or a transition state as depicted. Loss of labeled ethylene from this species regenerated $2'\text{-trans}$ and 2 and completes one intermolecular exchange event. While this mechanism is attractive owing to its simplicity, the intermediate 3-trans is likely to be highly disfavored since the trans arrangement of the NHC and the methylidene is a high-energy prospect since they are both strong donors. It therefore is more plausible to describe this point on the reaction coordinate as a transition state (i.e., 3-trans^\ddagger), although this begins to resemble a ruthenacyclohexane-type structure, for which there is no evidence in the literature in existing discussions on olefin metathesis mechanisms. (The observation that 2 decomposes in the presence of ethylene by pathways that yield propene, and no C_5 or C_2 products, argues against such structures.)²⁹

(26) (a) Lee, J. B.; Ott, K. C.; Grubbs, R. H. *J. Am. Chem. Soc.* **1982**, *104*, 7491. (b) Finch, W. C.; Anslyn, E. V.; Grubbs, R. H. *J. Am. Chem. Soc.* **1988**, *110*, 2406. (c) Anslyn, E. V.; Grubbs, R. H. *J. Am. Chem. Soc.* **1987**, *109*, 4880.
 (27) Feldman, J.; Davis, W. M.; Thomas, J. K.; Schrock, R. R. *Organometallics* **1990**, *9*, 2535.

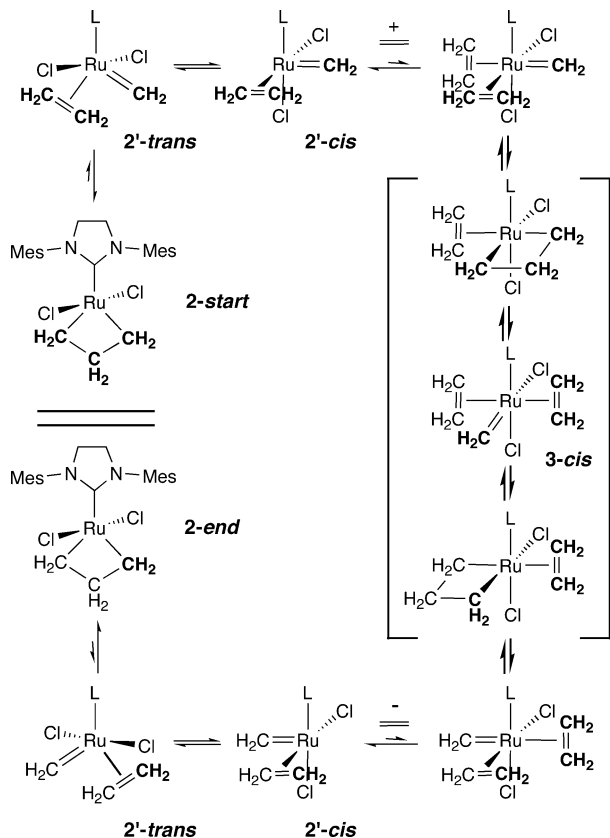
(28) Laidler, K. J. *Chemical Kinetics*, 3rd ed.; Harper and Row: New York, 1987; pp 129, 135.

(29) (a) McDermott, J. X.; White, J. F.; Whitesides, G. M. *J. Am. Chem. Soc.* **1976**, *98*, 6521. (b) McDermott, J. X.; Wilson, M. E.; Whitesides, G. M. *J. Am. Chem. Soc.* **1976**, *98*, 6529. (c) Jacobson, D. B.; Freiser, B. S. *Organometallics* **1984**, *3*, 513. (d) Grubbs, R. H.; Miyashita, A. *J. Am. Chem. Soc.* **1978**, *100*, 7418.

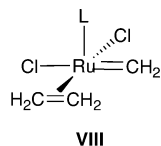
Scheme 4



Scheme 5



Alternatively, the mechanism depicted in Scheme 5 is somewhat more complex but invokes *cis*-disposed chlorides akin to those recently observed experimentally in model olefin-alkylidene compounds based on the Grubbs generation 2 catalyst framework.⁹ In these *cis*-chloride intermediates, one of the chloride ligands migrates to the position *trans* to the NHC ligand, as opposed to the position *trans* to the alkylidene moiety. While a *cis*-chloride mechanism with the chlorides *cis*-disposed in this latter arrangement (i.e., **VIII**), is viable, such structures have been computed to invariably minimize to *cis*-chloride structures with a Cl ligand *trans* to the NHC, and no experimental models have been found.



Thus, as shown in Scheme 5, *2'*-*trans* isomerizes into *2'*-*cis*

via a sequence of Berry pseudorotations, and then picks up an unlabeled ethylene ligand to form the putative 18-electron species key to the associative exchange. To complete the exchange without violating microscopic reversibility, a sequence of methathesis-like steps (depicted inside the square brackets) rapidly occurs, proceeding through the *cis*-chloride isomer of **3**. Upon regeneration of the 18-electron bisethylene species, exchange has been completed. Loss of ethylene regenerates *2'*-*cis/trans* and ruthenacyclobutane **2**.

Conclusions

The degenerate exchange of free ethylene with the methylene units of the 14-electron ruthenacyclobutane **2** is a process directly related to the bond breaking and forming steps in the olefin metathesis reaction catalyzed by generation 2 Grubbs catalyst. As such, the kinetic information provided here is the first glimpse of the kinetic and thermodynamic parameters associated with these key steps in this process, previously unobtainable owing to their kinetic invisibility in the Grubbs generation 1 and 2 catalyst systems. The observation of an associative exchange of ethylene into this parent ruthenacyclobutane has implications for the mechanism of productive metathesis, but caution must be exercised in generalizing these results to the more substituted ruthenacyclobutanes endemic to higher metathesis processes. The unsubstituted ruthenacyclobutane **2**, for example, is the thermodynamically most stable member of this family, and its behavior may be substantially different than substituted analogues. It should also be noted that the low-temperature regimes used to make these measurements may disfavor a competing dissociative mechanism with a large positive entropy of activation. Nonetheless, the observed kinetic behavior is intriguing, and to the extent that catalyst speciation in metathesis processes mediated by **1** and evolving ethylene may pool in **2**, a detailed understanding of the mechanisms by which **2** undergoes exchange with olefins is of interest. The proposals put forward in Schemes 4 and 5 are reasonable and consistent with our observations, but affirmation of one or the other await further investigations, particularly computational studies. Further kinetic studies on more substituted ruthenacyclobutanes¹⁴ are of obvious priority; such studies are currently in progress.

Experimental Section

General. Argon filled Innovative Technology System One dry boxes were used to store air and moisture sensitive compounds, and for manipulation of air-sensitive materials. Reactions were performed either on a double manifold vacuum line using standard Schlenk techniques or under an argon atmosphere in the dry box for small-scale reactions.

Glassware used in anhydrous reactions was stored in a hot oven (110 °C) overnight or flamed dried prior to immediate use, and then transferred to the dry box. Where applicable, cooling baths consisting of liquid nitrogen (−196 °C) dry ice/acetone (−78 °C), dry ice/acetonitrile (−44 °C), and heavily salted acetone/water/ice (−15 °C) mixtures were used to maintain low-temperature conditions.

Nuclear magnetic resonance spectroscopy (^1H , ^{11}B , ^{13}C , ^{19}F , ^{31}P , HMQC, EXSY, and COSY) was performed on Bruker AC-200 (^1H , 200.134 MHz), AMX 300 (^1H 300.138, ^{19}F 282.371 MHz), and BAM-400 (^1H 400.134 MHz, ^{13}C 100.614 MHz, ^{11}B 128.377 MHz, ^{31}P 161.975 MHz). All ^1H and ^{13}C spectra were referenced to Me_4Si at 0 ppm through the residual ^1H signal(s) of the deuterated solvents used. For most compounds, ^{13}C NMR resonances were assigned using the HMQC pulse sequence. ^{11}B NMR spectra were referenced to an external standard of $\text{BF}_3 \cdot \text{Et}_2\text{O}$ in C_6D_6 at δ 0.0 ppm prior to the acquisition of the spectrum. ^{19}F NMR spectra were referenced externally to C_6F_6 in C_6D_6 at δ −163 ppm relative to CFCl_3 at δ 0.0 ppm. ^{31}P NMR spectra were referenced to an aqueous external standard of 85% H_3PO_4 in D_2O at δ 0.0 ppm. Temperature calibration for low-temperature NMR experiments was achieved by monitoring the ^1H NMR spectrum of pure methanol. Exchange NMR spectroscopy experiments (EXSY) were acquired in phase-sensitive mode using the Bruker pulse program *noesytp*. A shifted sine-bell window function was applied to the raw data set in both dimensions. The spectra were recorded with a sweep width of 11 ppm, 1024 data points in the *F2* direction, and 256 increments in the *F1* direction. For quantitative experiments 8 scans were collected for every spectrum. T_1 measurements were performed on the resonances of interest and a delay (*d1*) of $5 \times T_1$ between single acquisitions was used, taking as a reference the longest relaxation time. In the case of metallacyclobutane **2**, $5 \times T_1$ corresponded to 3 s. Short mixing times (τ_m) between 10 and 40 ms were used for the extraction of kinetic data. This set of parameters produced a total acquisition time of ca. 110 min for each experiment depending on the mixing time used. Integration of the cross-peaks of interest was performed using the Bruker TopSpin software.

Complex **1**¹⁰ and metallacyclobutanes **2** and **2**- $^{13}\text{C}_3$ ¹¹ were prepared as outlined before. Solvents were purified by standard methods where necessary. Ethylene gas was purchased from Matheson and passed through an Oxysorb-W purification column before introduction to the reaction vessel. Stoichiometric NMR tube-scale gas additions were carried out using gastight syringes and considering ideal gas behavior at room temperature as described previously.¹⁰

Kinetics of Olefin Exchange. The kinetics of the degenerate exchange of ethylene between **2** and **2**- $^{13}\text{C}_3$ were carried out using a small NMR scale, gas addition setup connected to a digital VAP 5 vacuum gauge and adapted for a J-Young tube. In a typical experiment, 12 mg (8.3 μmol) of complex **1** were weighed into a J-Young tube and dissolved in 600 μL of CD_2Cl_2 , which contained a measured amount of 1,4-dimethylbenzene as an internal standard in a glovebox. The tube was connected to the gas addition setup and frozen in liquid nitrogen (fully submerged), after which the system was fully evacuated (10^{-3} – 10^{-4} Torr). The tube was then closed and left to warm to room temperature. The freeze–pump–thaw cycle was repeated once more, and then the tube was closed under full static vacuum. $^{13}\text{C}_2\text{H}_4$ was then admitted into the system, by carefully opening the regulator until an ethylene pressure of ca. 40 Torr was reached (8.25 mL in the internal bulb, ca. 2.2 equiv of ethylene) and the regulator was closed. After 15–20 min, complete mass transfer took place, and the tube was closed and defrosted in a dry ice/acetone bath at −78 °C. Before acquisition of the corresponding NMR spectrum, the tube was quickly shaken and placed back into the cold bath to ensure complete mixing of the reactants. The tube was then placed into the precooled NMR probe

(−50 °C) and monitored until complete conversion to the labeled metallacyclobutane **2**- $^{13}\text{C}_3$ took place.

After conversion took place (on average 1.5 to 2 h), *n* equivalents of C_2H_4 (with *n* = 10, 20, 25, 30, and 35) were added to the J-Young tube at liquid nitrogen temperature. The tube was kept at this temperature and taken to the NMR facility where it was defrosted at −78 °C in a dry ice/acetone bath immediately prior to insertion into the magnet, which was precooled at −50 °C. The decay of **2**- $^{13}\text{C}_3$ into **2** was monitored automatically at different intervals depending on the amount of equivalents of C_2H_4 added, by following the disappearance of the labeled β -hydrogens resonance at δ −2.6 ppm. T_1 measurements were performed for the hydrogens in the metallacyclobutane and a delay of $5 \times T_1$ between single acquisitions was used (*d1* = 3 s) and the same spectral window was integrated consistently. Under these conditions a pseudo-first-order regime was generated for *n* = 20, 25, 30, and 35 and the respective plots of $\ln([\text{Ru}]/[\text{Ru}]_0)$ versus time were obtained. Each measurement was performed twice, the duplicate results for k_{obs} being the same within 5%. For *n* = 10 the system did not follow first-order decay and rather, a reversible first-order equilibrium was established. Therefore this measurement was not utilized in subsequent calculations. From these measurements, a plot of k_{obs} versus $[\text{C}_2\text{H}_4]$ was generated and an average k_{exchange} of $8.1 \times 10^{-4} \text{ L mol}^{-1} \text{ s}^{-1}$ was obtained at −50 °C. The actual concentration of ethylene was obtained at the end of each single measurement by integration of the C_2H_4 signal at 5.4 ppm against the internal standard, using a *d1* delay of 150 s (4 scans for total acquisition).

The experiments described above were repeated at different temperatures to allow the construction of an Eyring plot and extract the corresponding activation parameters. However, to obtain accurate numbers, the ethylene concentration needed to remain constant during the different measurements. Because of the gaseous nature of C_2H_4 its concentration in solution varies greatly with temperature, particularly at near saturation conditions. Therefore, a solubility study was conducted in parallel using CD_2Cl_2 as a blank solution (containing 1,4-dimethylbenzene as an internal standard), and adding variable amounts of ethylene. The concentration of gas in solution was then monitored as a function of temperature. By performing these experiments it was found that at $[\text{C}_2\text{H}_4] = 0.37 \text{ M}$, the variation of concentration with temperature (between −70 and −45 °C) was minimal (less than 5%). This concentration corresponds to ca. 20 equiv of C_2H_4 with respect to **1**. An Eyring plot ($\ln(k_i/T)$ versus $1/T$) was then constructed ($T = -69.3$, −60.2, −50.8, and −45.6 °C) using this amount, which allowed the extraction of the activation parameters $\Delta H^\ddagger = 13.2 \text{ kcal mol}^{-1}$ and $\Delta S^\ddagger = -15 \text{ eu}$. Accurate temperatures in the NMR probe were obtained using a methanol thermometer immediately after the respective run.

Acknowledgment. This work was funded by the Natural Sciences and Engineering Research Council (NSERC) of Canada in the form of a Discovery Grant to W.E.P. We thank Materia Inc. (Pasadena) for a generous gift of Grubbs second-generation catalyst. P.E.R. thanks the University of Calgary for a Dean's Special Doctoral Scholarship. The authors thank Prof. Robert Grubbs (Caltech) for sharing unpublished results.

Supporting Information Available: Tables of ^1H and ^{13}C NMR data for comparable ruthena- and metallacyclobutanes, and a speciation plot for ethylene exchange at low $[\text{CH}_2=\text{CH}_2]$. This material is available free of charge via the Internet at <http://pubs.acs.org>.

JA0675245